

## Efficient numerical simulation of granular matter using the Bottom-To-Top Reconstruction method

Thomas Schwager and Thorsten Pöschel

Centrum für Muskuloskeletale Chirurgie, Charité, Campus Virchow-Klinikum,  
Augustenburger Platz 1, 13353 Berlin, Germany

### Abstract

The numerical simulation of granular systems of even moderate size is a challenging computational problem. In most investigations, either Molecular Dynamics or Event-driven Molecular Dynamics is applied. Here we show that in certain cases, mainly (but not exclusively) for static granular packings, the Bottom-to-top Reconstruction method allows for the efficient simulation of very large systems. We apply the method to heap formation, granular flow in a rotating cylinder and to structure formation in nano-powders. We also present an efficient implementation of the algorithm in C++, including a benchmark.

### Introduction

The intention of numerical particle simulations of granular matter is (at least) two-fold. First, simulations are frequently helpful to explain experimental results, that is, to improve our understanding of the static and dynamic behavior of granular matter and to improve its corresponding theoretical description. Second, yet more important, particle simulations may be helpful for engineers to construct or optimize technical devices to handle and process granular materials. Having a reliable numerical method at hand, the prediction of granular matter behavior is even possible if there is no theoretical description due to our limited understanding or for more fundamental reasons [11].

The main problem in applying particle simulations as a standard tool in engineering is the enormous consumption of computational power (see [32] for an overview). The most universal method for particle simulation is *Molecular Dynamics* (MD), also called Discrete Elements Method, where Newton's equation of motion is solved simultaneously for all particles of the system. The knowledge of the interaction forces is sufficient, in principle, to simulate any granular assembly with arbitrary boundary conditions. Unfortunately, due to the large stiffness of the particle, expressed by the Young modulus of the material, MD simulations of granular matter require a very small integration time step which implies high computational costs. At present, for systematic investigations of systems over a longer period, the number of particles is restricted to significantly below  $10^5$ . On the other hand, even a relatively small container as used for experimental investigations comprises much more particles, sometimes billions.

The simulation may be accelerated considerably by assuming that each contact of particles is an instantaneous event, that is, the duration of contacts vanishes and in the entire system at any time only two particles are in contact. Under this condition, *Event-*

*driven MD* (EMD) may be applied. Here, instead of integrating Newton's equation, the evolution of the system is determined by the sequence of particle collisions, where the postcollision velocities are computed as functions of the precollision velocities and the coefficients of restitution which are functions of the impact velocity themselves, see [32]. In the limit of very dilute systems of stiff particles, called granular gases, both algorithms, MD and EMD, deliver identical results. Using desktop computers, at present we can simulate about  $10^7$  particles using EMD, however, the above-mentioned condition of EMD does obviously not allow for its application as a general simulation tool. EMD, in principle, is not suited to simulate systems where particles contact each other over a non-vanishing period of time.

A complementary approach is the *Bottom-To-Top Reconstruction* method (BTR). Here the simultaneous numerical integration of the  $N$ -particle system is approximated by the sequential numerical integration of a one-particle system with complex boundary conditions. Similar as EMD, BTR is also much more efficient than MD at the price of a restricted applicability, see Sec. 7. While the main precondition of EMD is vanishing contact time, for BTR we have to require that a particle having arrived in a stable position does not leave this position anymore. That is, complementary to EMD, BTR requires persistent contacts. There are cases when the application of BTR leads to unphysical results, however, if the algorithm is applicable, it leads to a vast increase of numerical efficiency; at present we can simulate systems of many millions particles on a desktop computer. The range of its applicability and benchmarks of the algorithm are discussed at the end of this article.

## 2 Bottom-to-top Reconstruction

The idea of BTR goes back to Visscher and Bolsterli [36] who suggested an algorithm that allows for the fast simulation of large static granular packings. The fundamental idea of their method is to consider the motion of the particles sequentially, unlike in MD simulations, where the coupled system of Newton's equations of motion is solved for all particles simultaneously.

The deposition of the particles of a granular packing, e.g., a heap on the plane  $(x, y, 0)$ , proceeds as follows: the first particle is inserted at position  $(x_1^{\text{init}}, y_1^{\text{init}}, z_1^{\text{init}})$ . The coordinate  $z_1^{\text{init}}$  should be larger than the expected final height of the heap, the coordinates  $x_1^{\text{init}}$  and  $y_1^{\text{init}}$  can be chosen at random (particles are scattered over a certain area) or can be fixed, e.g.,  $(x_1^{\text{init}}, y_1^{\text{init}}) = (0, 0)$ , to simulate the build-up of a heap from a point source. The particle then falls until it touches the ground at  $(x_1^{\text{init}}, y_1^{\text{init}}, R_1)$ . At this position the particle remains fixed. Then the second particle is inserted at position  $(x_2^{\text{init}}, y_2^{\text{init}}, z_2^{\text{init}})$ . It falls down until it touches either the ground at  $(x_2^{\text{init}}, y_2^{\text{init}}, R_2)$  or the first particle, whatever happens first. If it touches the ground it remains fixed there just like the first particle. If it, however, touches the first particle, it rolls down its surface in the downslope direction until it either touches the ground (if  $R_2 \geq R_1$ ) where it remains fixed or (if  $R_2 < R_1$ ) until it loses contact at  $z_2 = R_1$  when both centers are at the same height. From there it falls to the ground where it remains fixed. The next particles are treated likewise. A particle remains fixed if it either touches the ground or if it attains a local minimum where it is supported by two (in two dimensions) or three (in three dimensions) other already fixed particles.

Thus, each particle moves according to a set of rules from one state to the next. In this sense the algorithm belongs to the class of event-driven algorithms.

In Fig. 1 the algorithm is sketched for a two-dimensional system. The moving particle is drawn with a dotted line, fixed particles are drawn with a solid line. The algorithm by Visscher and Bolsterli [36] was later improved and generalized, e.g., [17–19] and also applied to certain dynamical systems [4, 5], see below.

The BTR algorithm is not exact, that is, it does not solve the coupled set of Newton's equations for the dynamics of the many-particle systems. Instead, there are three major simplifying assumptions

1. The motion of each particle  $i$  is computed with the wall and the other already-deposited particles  $j = 0, \dots, i - 1$  considered as fixed obstacles. The positions of the particles  $j = 0 \dots i - 1$  are not influenced by the motion of the new particle  $i$ . Thus, the trajectory of each particle is computed while taking gravity as the only driving force into account. The other particles  $j = 0 \dots i - 1$  and the wall establish the (complicated) boundary conditions to this motion. This

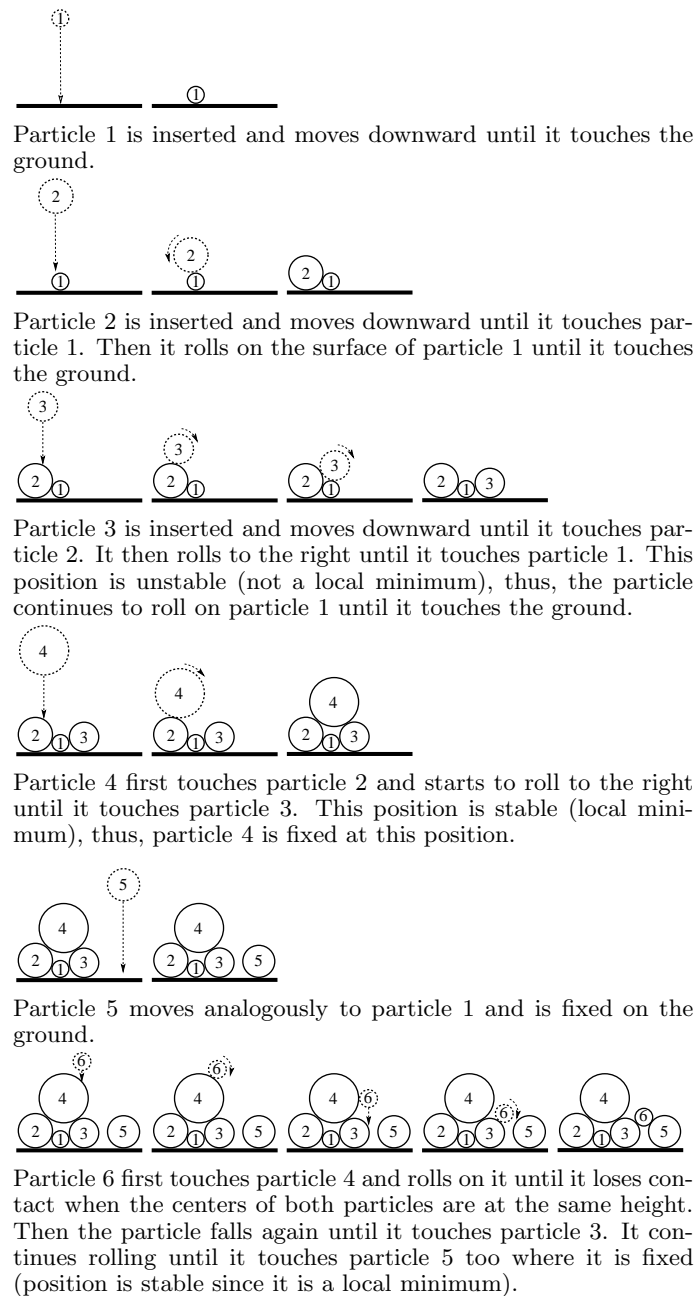


Figure 1: Sketch of the BTR algorithm

way, the system of Newton's equation for the  $N$ -body system is decoupled and  $N$  single-particle equations are solved instead.

2. Collisions of particle  $i$  with the wall or with other particles are assumed to be perfectly inelastic.
3. The time dependence of the particles' motion is disregarded.

These simplifications increase the efficiency of the simulation significantly. Jullien et al. [20] were able to simulate packings of up to  $10^8$  particles using this algorithm. The simplifications restrict the applicability of BTR to a rather small class of problems, see Sec. 7. If applicable, however, BTR is a very efficient simulation tool.

### 3 Implementation of the BTR algorithm

The BTR algorithm allows for a very efficient numerical simulation. We briefly explain the implementation for the simulation of a two-dimensional heap which is the simplest application of BTR and restrict ourselves to the simulation of a two-dimensional system of poly-disperse particles. The extension to three dimensions is straightforward. A more detailed explanation can be found in [32] and the full source code of our program is available at [1].

To compute the deposition of the  $n$ th particle, we do not need the positions of all  $n - 1$  previously deposited particles. Instead, it is sufficient to know the positions of particles that can come into contact with particle  $n$ , i.e., particles at the surface of the heap. This simplification is always justified for two-dimensional systems, whereas for three-dimensional systems it is only justified if the ratio between the largest and smallest radii of the particles in the system does not exceed the Apollonian ratio  $r_A \equiv R_{\max}/R_{\min} = \sqrt{3}/(2 - \sqrt{3}) \approx 6.46$ . Otherwise the smaller particles can fall into the gaps between the larger particles and thus, in principle, interact with all particles of the heap. In this case, we cannot exclude any pair interactions à priori. A natural choice of radii within  $(R_{\min}, R_{\max})$  is to assume that the total mass of particles from the interval  $(R, R + dR)$  is constant regardless of  $R$ . Such a distribution can be obtained from equi-distributed random numbers  $z \in [0, 1)$  using the transformation [32, 33]

$$R_i = \frac{R_{\min} R_{\max}}{R_{\max} - z(R_{\max} - R_{\min})}. \quad (1)$$

We store the indices of the particles at the surface in the container `surface` of type `map<double,int>` where the key is the their  $x$ -coordinate.

Consider the deposition of particle  $n$ . If  $n$  is not in contact with any other particle it moves downward until it touches the ground or another particle. Apart from the ground plane all particles on the surface of the heap whose centers belong to the interval  $(x_n - R_n - R_{\max}, x_n + R_n + R_{\max})$  are potential contact partners, see Fig. 2. The container `map` allows to very efficiently iterate through these contact candidates.

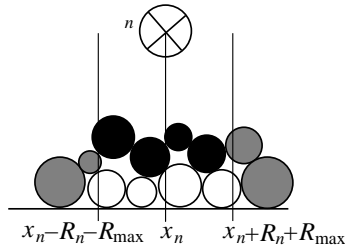


Figure 2: The centers of the contact candidates of the falling particle  $n$  (crossed circle) belong to the interval  $(x_n - R_n - R_{\max}, x_n + R_n + R_{\max})$  (black filled circles). The other surface particles are drawn gray, particles which are not part of the surface are drawn hollow

For all contact candidates  $i$  that are located below the particle to be deposited, we check if and at which

height  $yy$  both particles touch, disregarding for the moment possible interference from other particles, that is, we check whether

$$yy = y_i + \sqrt{(R_n + R_i)^2 - (x_i - x_n)^2}, \quad (2)$$

has a real solution and determine the maximum of this expression for all  $i$  (see Fig. 3). To determine the desired contact point also a possible contact with the ground must be taken into account. Particle  $n$  is now

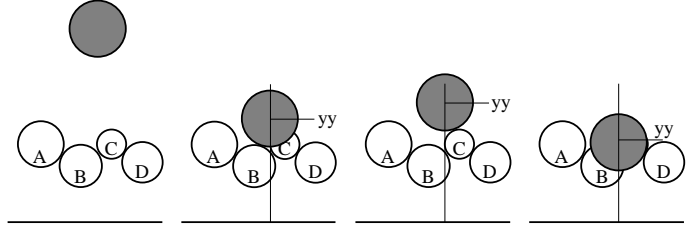


Figure 3: For each of the candidates  $A-D$  (drawn in black in Fig. 2) we determine the vertical coordinate  $yy$  of a possible contact. The highest contact is with candidate  $C$ , therefore,  $C$  is the contact partner we are looking for

moved downward to contact its partner particle or the ground. In the latter case, its new position is stable by definition and its deposition is accomplished. If, however, the particle meets another particle first, its new position cannot be stable. Instead it continues its motion by rolling down the surface of the contact partner until it comes into contact with the wall or with another particle, or it continues to fall down, as sketched in Fig. 1.

Similar as described above, again all possible candidates for the additional contact partner are determined, i.e., all particles that may be contacted by particle  $n$  while maintaining contact to its present partner  $p$ . The new particle rolls to the left if  $x_n < x_p$  or to the right otherwise. Candidates for the contact are particles whose  $x$ -coordinate is in the interval  $x_p \dots x_p \pm (R_p + 2R_n + R_{\max})$ , see Fig. 4. Again the index range of the candidate partners can be obtained easily from the `map surface`.

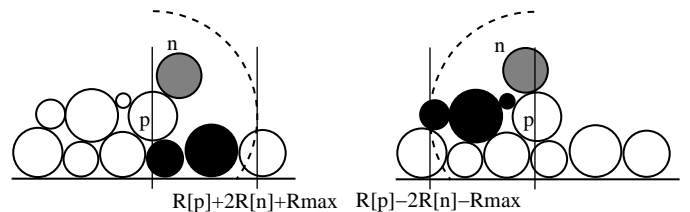


Figure 4: The centers of the candidates for the second partner particle are located within the circle of radius  $r = R_p + 2R_n + R_{\max}$  around  $x_p$ . Depending on the relative position of the particles  $n$  and  $p$  the circle can be reduced to a half circle. The particles represented by filled circles are the candidates

We investigate the possible contact of particle  $n$  rolling down the surface of particle  $p$  with each candidate  $i$  separately, disregarding all other particles for the moment, that is, we seek real solutions  $\vec{r}_n^i \equiv (x_n^i, y_n^i)$

of the system

$$|\vec{r}_n^i - \vec{r}_p| = R_n + R_p \quad (3)$$

$$|\vec{r}_n^i - \vec{r}_i| = R_n + R_i,$$

for contacts between particles  $n$ ,  $p$  and  $n$ ,  $i$  and of the system

$$|\vec{r}_n^w - \vec{r}_p| = R_n + R_p \quad (4)$$

$$y_n^w = R_n.$$

for a possible contact between particles  $n$  and  $p$  and of  $n$  with the floor. If these systems have real solutions the new position of particle  $n$  is determined by the solution  $\vec{r}_n^i \equiv (x_n^i, y_n^i)$  or  $\vec{r}_n^w \equiv (x_n^w, y_n^i)$  with the largest maximum vertical component, provided,  $y_n^i$  or respectively  $y_n^w$  is larger than  $y_p$ . In this case we found a new position of particle  $n$ . We now check for stability (i.e. if the particle is supported both from the right of his center and from the left). If it is stable the deposition of the particle is finished, otherwise particle  $i$  assumes the role of particle  $p$  and particle  $n$  continues to roll on its surface. If no candidate is found before particle  $n$  reaches  $y_n = y_p$ , it loses contact with  $p$  and again falls vertically downward, see last line in Fig. 1. This procedure is repeated until a stable position of particle  $n$  is found.

When the stable position of  $n$  is found, the map **surface** is updated. First,  $n$  is recorded as a member of the map since it became part of the surface. Second, after depositing  $n$ , other particles may be screened, such that no further particles may come into contact with them. Consequently, these particles are not members of the surface anymore and are removed from **surface**, see Fig. 5.

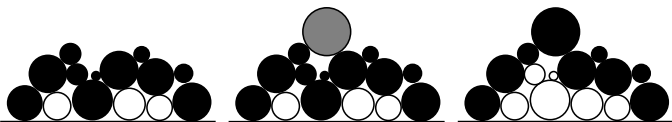


Figure 5: *Left*: surface particles before the deposition of the new particle (drawn gray). *Center*: a new particle is deposited. *Right*: corrected list of surface particles

The description of the algorithm and the sketch of the implementation is now complete. Figure 6 shows snapshots of a growing heap. The particles which are part of the surface are drawn filled.

Since particles in the process of deposition can contact only the particles at the surface, unlike as in MD the computational complexity of depositing a particle  $n$  does not grow with the number of already deposited particles,  $\mathcal{O}(n)$  but it increases with  $\mathcal{O}(n^{1/2})$  in 2d or with  $\mathcal{O}(n^{2/3})$  in 3d which is the reason for the computational power of BTR. We discuss the efficiency of the algorithm below in Sec. 7.

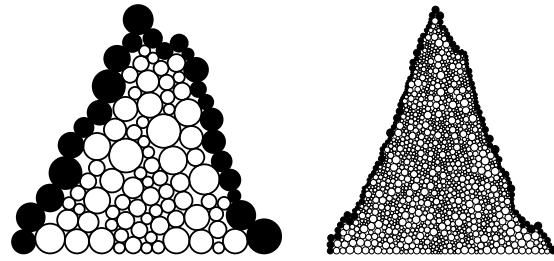


Figure 6: Snapshots of the growing heap. The number of particles is  $N = 100$  and  $N = 1400$

#### 4 Example: Stratification in a Sand Heap

When a heap of particles is created by sequentially depositing particles of different size, size segregation (stratification) is observed, which is caused by different angles of repose for large and small particles [10, 22, 37, 38]. The particles form stripes as shown in Fig. 7. In three dimensional dunes and ripples, other

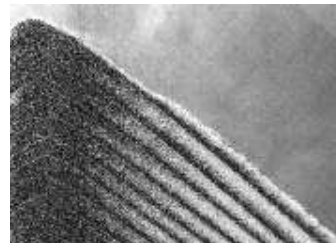


Figure 7: Formation of stripes in a heap consisting of particles of different properties (experimental result). The figure was taken from [15]

more complex stratification patterns are observed [2]. This effect has been studied and modeled extensively, e.g., in [8, 9, 12–14, 16, 21, 23–27, 27–30]. Similar structures have been observed in sand overflow by wind or water [35].

Figure 8 shows a heap of  $N = 10^6$  particles of two different radii. The effect of stratification is visible in the close-ups. The small particles are drawn filled.

#### 5 Sedimentation of Nano-Powders

The BTR-method can be generalized to clusters of contacting particles. Here clusters are considered as perfectly rigid, that is, the particles belonging to a cluster do not change their relative positions. This idealized behavior may be adequate for cohesive nano-powders where the attractive surface forces exceed by far inertial forces, due to their enormous surface area per unit mass. The attracting force between particles in contact provides a mechanism which fixes particles to a position where they were first deposited. Also due to the surface forces, nano-powders are frequently very porous. In this section we describe briefly the application of BTR to coarsening of nano-powders in the process of repeated siphoning the material from one container into another. For a more detailed description see [34].

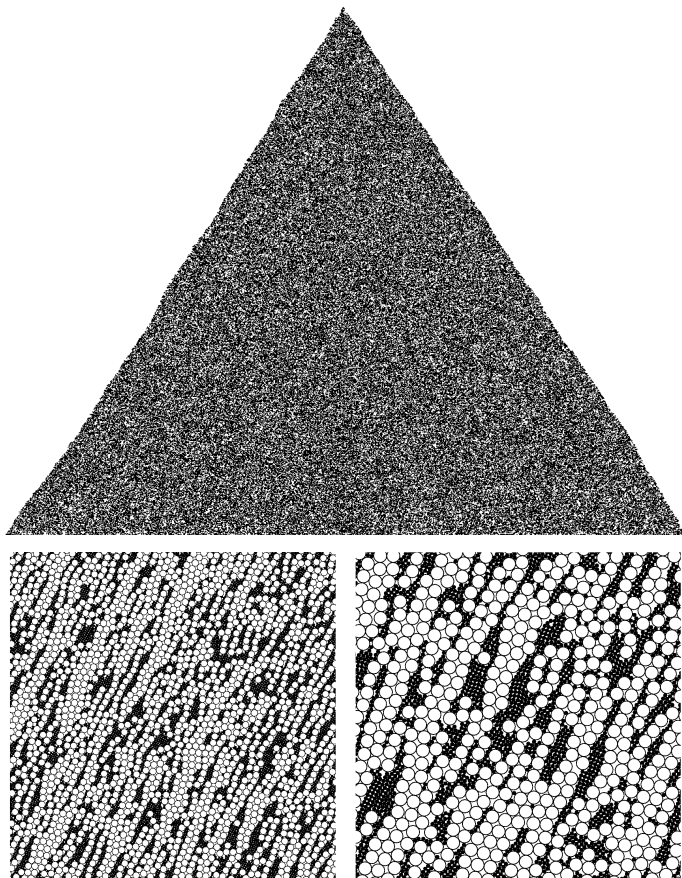


Figure 8: A heap consisting of  $N = 10^6$  particles of two different radii. Size segregation (stratification) can be seen in the close-ups

For clusters, the first step of the BTR algorithm is handled as for simple spheres: We determine the position of the falling cluster when one of its particles touches a particle of the sediment or the wall.

Rolling of the cluster on the already deposited heap particles is more complicated. Apart from situations discussed in Sec. 3 one is confronted with a large number of special cases whose discussion is outside the scope of this work [34].

For efficient simulation of both processes, falling and rolling, we need the *accessible surface* of the cluster, that is, those particles which due to geometry can come into contact with other particles or the floor. There are several efficient algorithms to determine this surface [31]. Fig. 9 shows an example cluster and its surface (filled circles). The holes in the surface are small enough to keep outside particles away from the inner particles. In our simulation of a coarsening nano-powder of  $N = 6 \cdot 10^6$  cohesive particles,  $R \in (0.9, 1.1)$ , initially the particles (or small clusters of a few particles) are placed into a rectangular container of length  $L = 8000$  limited by vertical walls. After the initial sedimentation due to standard BTR they are densely packed in the container (see Fig 10, left). To obtain a flat surface of the heap one has to insert the particles at random positions distributed uniformly over the length of the box. The material is now cut into square blocks of about  $50 \times 50$  average particle diameters. The blocks are decomposed into

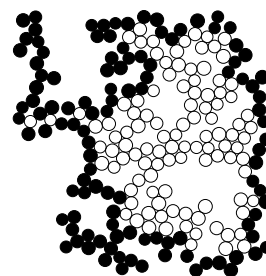


Figure 9: Typical cluster after a few disposition cycles. Dark circles represent surface particles. The surface is not contiguous, the gaps are, however, too small for outside particles to touch inner particles.

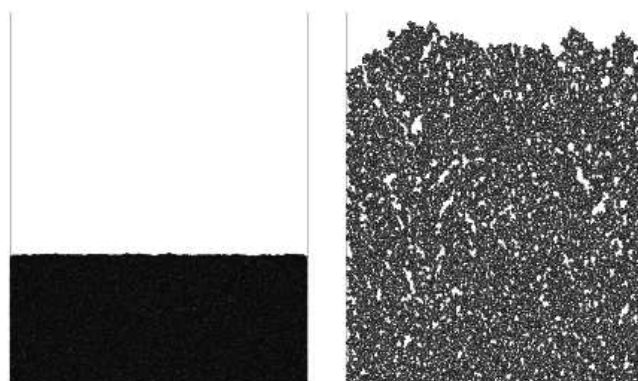


Figure 10: A heap of 6 million particles. Left: Particles deposited in clusters of 3. Right: After 18 redeposition cycles.

clusters of mutually contacting particles. Now these clusters are sedimented into the container. Figure 11 shows the average height  $\langle h \rangle$  of the material surface over the number of sedimentation cycles.

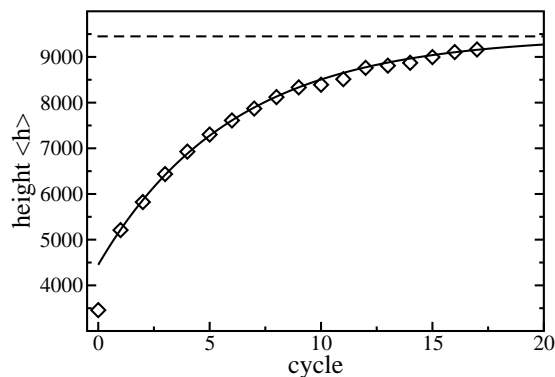


Figure 11: Average height of the heap vs number of disposition cycles. The solid line is the fit to an exponential function, the diamonds are the measured values.

This quantity was computed by cutting the box into narrow vertical strips and determining the height  $h$  of the highest particle in each strip. The height of the strip is now  $h + R$  where  $R$  is the radius of the highest particle. Averaging over all strips yields  $\langle h \rangle$ . The data points fit an exponential law of the form  $\langle h \rangle = 9450 - 5000 \exp(-n/6)$  with  $n$  being the cycle number. The initial height does not fit into this scheme. This is due to the fact that the initial heap is build up

from very small structures (clusters of size 3 in the example) while each later sedimentation cycle is done with structures of a typical size 50. Fig. 10 shows the heap after 18 sedimentation cycles.

## 6 Dynamic Simulations

BTR cannot be applied directly to the simulation of dynamic processes since due to the main principle of this algorithm, deposited particles cannot leave their positions anymore. A very restricted class of dynamical systems can be simulated, however, if we partition the dynamics into alternating steps of collective motion and sequential deposition [19].

For the example of granular flow in a partially filled, slowly rotating cylinder, the partition of the (continuous) dynamics is [4, 5] (see Fig. 12):

1. *initialization*: Place the particles at random inside of the container.
2. *collective motion*: The positions of all particles follow the motion of the container for a small time step  $\Delta t$ .
3. *Preparation of the current time step*: Increase the  $y$ -coordinate of all particles by a constant, e.g.,  $R_{\text{cyl}}/10$ , with  $R_{\text{cyl}}$  being the cylinder radius.
4. *BTR*: Apply BTR to the particles in sequence of increasing  $y$ -coordinate.
5. *Loop*: Increase the system time by  $\Delta t$  and continue with step 2.

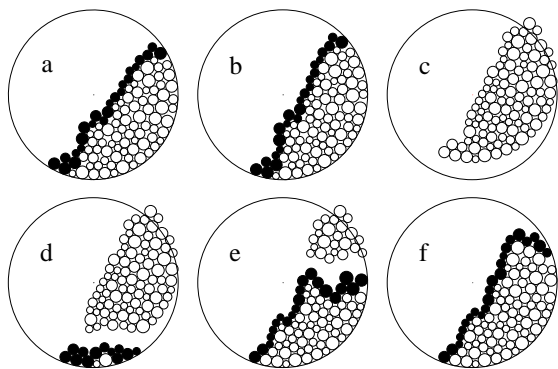


Figure 12: Dynamic BTR for the example of a slowly rotating cylinder. (a) The system at time  $t$ . (b) The cylinder is rotated (angle of rotation appears exaggerated). (c) All particles are lifted by  $R_{\text{cyl}}/10$ . (d, e) BTR, (f) Situation at time  $t + \Delta t$  when all particles are deposited

Figure 13 shows a snapshot of a simulation of  $N = 10^6$  particles of different radii  $R_i \in (0.1, 1)$  cm in a cylinder of radius 70 cm. The radii are chosen randomly in such a way that the total mass of all particles from the interval  $(R, R + dR)$  is constant regardless of  $R$ . We notice that the small particles are concentrated close to the center of the cylinder. This effect, which is observed also experimentally, was found in simulations in [4, 6].

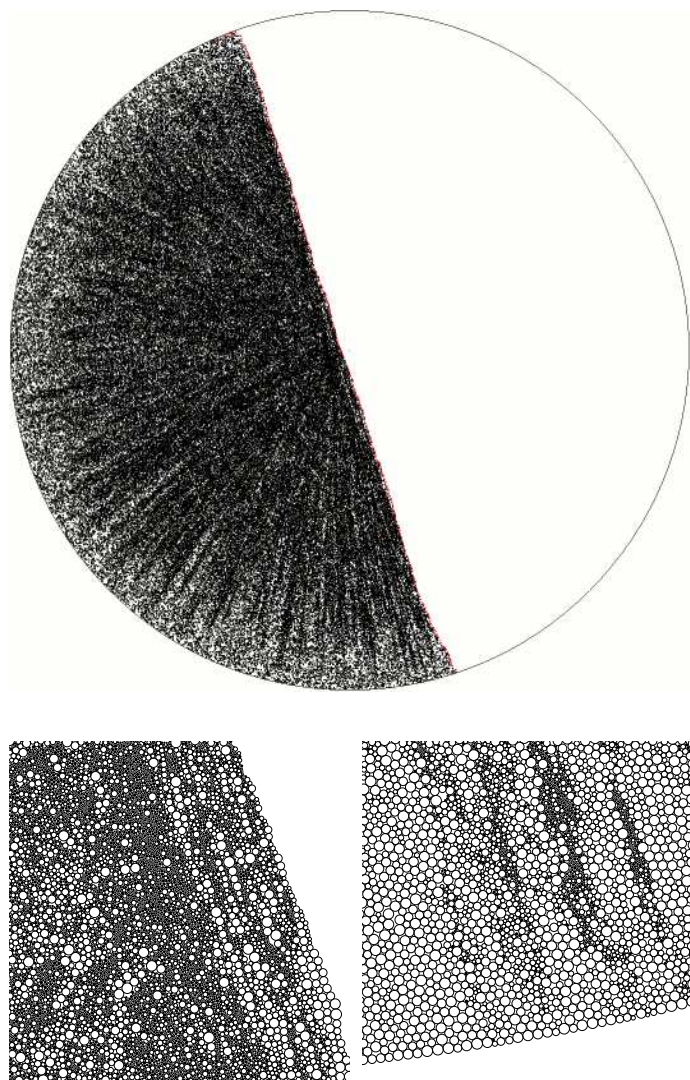


Figure 13: Snapshot of a slowly rotating cylinder filled with  $N = 10^6$  granular particles and close-ups. After one revolution consisting of 100 deposition steps, size segregation is clearly visible. For better presentation in the top figure only 30% of the particles are drawn

## 7 Benchmarks of the Implementation and Critical Analysis of the Model

BTR-simulations perform in general much faster than regular MD. Although BTR was successfully applied to various large granular systems, this method is not universal, and there are cases where physically incorrect behavior is observed [3].

A deposited particle does not move under the influence of particles deposited later, even if the particle suffers (in the realistic system) violent collisions. The motion of the particles is, thus, not governed by Newton's equation of motion. Instead, each single grain performs an overdamped motion in a complicated potential landscape comprising the already deposited grains. This is equivalent to disregarding inertial forces and moments. Even from a very basic and intuitive concept of classical mechanics it is clear that this algorithm cannot describe the granular many-body problem in a general way. It should be

regarded as a compromise between computing power requirements and realistic description of physical reality. Figure 14 demonstrates that BTR may lead to non-physical descriptions.

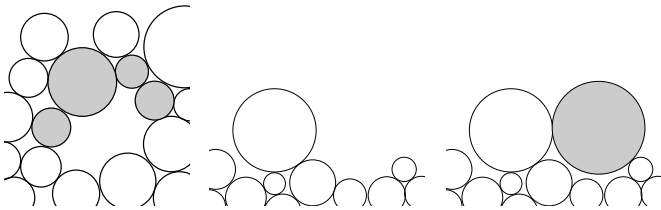


Figure 14: *left*: The configuration of particles is physically possible and stable, but cannot be generated by BTR since none of the gray particles is in a stable position without the others, i.e., none of them could be deposited first. *middle and right*: BTR may generate this sequence, although it is not realistic since the configuration on the right-hand side is unstable

Nevertheless, *if* BTR is applicable, it leads to a great increase of performance as compared with MD. Figure 15 shows the CPU time to deposit a heap of  $N$  particles, using a desktop computer (Intel Pentium 4, 3GHz). The program code is available at [1].

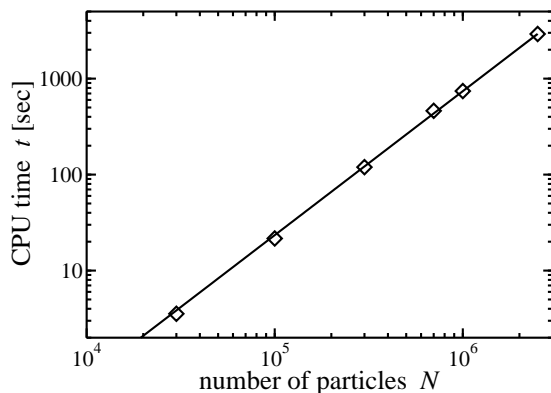


Figure 15: CPU time to build a heap of  $N$  particles using BTR. The data points (diamonds) are in close agreement with a power-law  $t \propto N^{3/2}$  (solid line) as discussed in the text

The algorithm may yield satisfactory results when treating systems where the boundary conditions change only very slowly. In such cases MD is frequently inefficient. In particular, for problems where the computation of the trajectories of individual particles is less important, the algorithm can be seen as a good compromise between efficiency and precision of the result.

## Acknowledgments

We thank Dietrich Wolf for discussion on the simulation of nano-powders. This work was supported by German Science Foundation via grant Po472/10-1.

## References

[1] The source code of the described implementation of BTR can be obtained at <http://bioinf.charite.de/cgd/>.

- [2] J. R. Allen. Asymmetrical ripple marks and the origin of cross-stratification. *Nature*, 194:167, 1962.
- [3] G. C. Barker, A. Mehta, and M. J. Grimson. Comment on “three-dimensional model for particle size segregation by shaking”. *Phys. Rev. Lett.*, 70:2194, 1993.
- [4] G. Baumann, I. János, and D. E. Wolf. Particle trajectories and segregation in a two-dimensional rotating drum. *Europhys. Lett.*, 27:203, 1994.
- [5] G. Baumann, I. M. János, and D. E. Wolf. Surface properties and flow of granular material in a 2d rotating drum model. *Phys. Rev. E*, 51:1879, 1995.
- [6] G. Baumann, E. Jobs, and D. E. Wolf. Granular cocktail rotated and shaken. *Fractals*, 1:767, 1993.
- [7] R. P. Behringer and J. T. Jenkins, editors. *Powders and Grains’97*, Rotterdam, 1997. Balkema.
- [8] T. Boutreux and P. G. de Gennes. Surface flows of granular mixtures: I. General principles and minimal model. *J. Physique I*, 6:1295, 1996.
- [9] T. Boutreux and P. G. de Gennes. Surface flow of granular mixtures. In Behringer and Jenkins [7], page 439.
- [10] R. L. Brown. The fundamental principles of segregation. *J. Inst. Fuel*, 13:15, 1939.
- [11] I. Goldhirsch. Granular gases: Probing the boundaries of hydrodynamics. In T. Pöschel and S. Luding, editors, *Granular Gases*, volume 564 of *Lecture Notes in Physics*, page 79. Springer, Berlin, 2001.
- [12] Y. Grasselli and H. J. Herrmann. Experimental study of granular stratification. *Granular Matter*, 1:43, 1998.
- [13] J. M. N. T. Gray and K. Hutter. Pattern formation in granular avalanches. *Cont. Mech. and Thermodyn.*, 9:341, 1997.
- [14] J. M. N. T. Gray and K. Hutter. Physik granularer Lawinen. *Physikalische Blätter*, 54:37, 1998.
- [15] J. M. N. T. Gray, Y. C. Tai, and K. Hutter. Shock waves and particle size segregation in shallow granular flows. In A. D. Rosato and D. L. Blackmore, editors, *IUTAM Symposium on Segregation in Granular Materials*, page 269, Dordrecht, 2000. Kluwer.
- [16] P. Y. Julien, Y. Q. Lan, and Y. Raslan. Experimental mechanics of sand stratification. In Behringer and Jenkins [7], page 487.

- [17] R. Jullien and P. Meakin. Simple three-dimensional models for ballistic deposition with restructuring. *Europhys. Lett.*, 4:1385, 1987.
- [18] R. Jullien and P. Meakin. Ballistic deposition and segregation of polydisperse spheres. *Europhys. Lett.*, 6:629, 1988.
- [19] R. Jullien and P. Meakin. Three-dimensional model for particle-size segregation by shaking. *Phys. Rev. Lett.*, 69:640, 1992.
- [20] R. Jullien, P. Meakin, and A. Pavlovitch. Particle size segregation by shaking in two-dimensional disc packings. *Europhys. Lett.*, 22:523, 1993.
- [21] J. Koepe, M. Enz, and J. Kakalios. Avalanche segregation of granular media. In Behringer and Jenkins [7], page 443.
- [22] J. Litwiniszyn and L. Ci-Tong. The phenomenon of segregation of grains of a loose medium when shaped in the form of a rotational half cone. *Bull. de L'Académie Polonaise des Sciences, Série des sciences techniques*, 11:169, 1963.
- [23] H. Makse, P. Cizeau, and H. E. Stanley. Possible stratification mechanism in granular mixtures. *Phys. Rev. Lett.*, 78:3298, 1997.
- [24] H. Makse, P. Cizeau, and H. E. Stanley. Modeling stratification in two-dimensional sandpiles. *Physica A*, 249:391, 1998.
- [25] H. A. Makse. Stratification instability in granular flows. *Phys. Rev. E*, 56:7008, 1997.
- [26] H. A. Makse, S. Havlin, P. C. Ivanov, P. R. King, S. Prakash, and H. E. Stanley. Pattern formation in sedimentary rocks: Connectivity, permeability, and spatial correlations. *Physica A*, 233:587, 1996.
- [27] H. A. Makse, S. Havlin, P. R. King, and H. E. Stanley. Novel pattern formation in granular matter. In L. Schimansky-Geier and T. Pöschel, editors, *Stochastic Dynamics*, Lecture Notes in Physics, page 319, Berlin Heidelberg New York, 1997. Springer.
- [28] H. A. Makse, S. Havlin, P. R. King, and H. E. Stanley. Spontaneous stratification in granular mixtures. *Nature*, 386:379, 1997.
- [29] H. A. Makse and H. J. Herrmann. Microscopic model for granular stratification and segregation. *Europhys. Lett.*, 43:1, 1998.
- [30] P. Meakin. A simple two-dimensional model for particle segregation. *Physica A*, 163:733, 1990.
- [31] J. O'Rourke. *Computational Geometry*. Cambridge University Class, 2000.
- [32] T. Pöschel and T. Schwager. *Computational Granular Dynamics: Models and Algorithms*. Springer, Berlin, Heidelberg, New-York, 2005.
- [33] W. H. Press, W. T. Vetterling, S. A. Teukolsky, and B. P. Flannery. *Numerical Recipes*. Cambridge University Press, Cambridge, 1988.
- [34] T. Schwager, D. Wolf, and T. Pöschel. in preparation.
- [35] H. C. Sorby. On the structures produced by the currents present during the deposition of stratified rocks. *The Geologist*, 2:137, 1859.
- [36] W. M. Visscher and M. Bolsterli. Random packing of equal and unequal spheres in two and three dimensions. *Nature*, 239:504, 1972.
- [37] J. C. Williams. The segregation of powders and granular materials. *Univ. Sheffield Fuel Soc. J.*, 14:29, 1963.
- [38] J. C. Williams. The segregation of particulate materials. A review. *Powder Techn.*, 15:245, 1976.